

Toward Astrometric Constraints on a Supermassive Black Hole Binary in the Early-Type Galaxy NGC 4472

J. M. WROBEL¹ AND T. J. W. LAZIO²

¹*National Radio Astronomy Observatory, P.O. Box O, Socorro, NM 87801, USA*

²*Jet Propulsion Laboratory, California Institute of Technology, 4800 Oak Grove Drive, Pasadena, CA 91109, USA*

(Received 2022 February 8; Accepted 2022 April 17)

Submitted to ApJ

ABSTRACT

The merger of two galaxies, each hosting a supermassive black hole (SMBH) of mass $10^6 M_{\odot}$ or more, could yield a bound SMBH binary. For the early-type galaxy NGC 4472, we study how astrometry with a next-generation Very Large Array (ngVLA) could be used to monitor the reflex motion of the primary SMBH of mass M_{pri} , as it is tugged on by the secondary SMBH of mass M_{sec} . Casting the orbit of the putative SMBH binary in terms of its period P , semimajor axis a_{bin} , and mass ratio $q = M_{\text{sec}}/M_{\text{pri}} \leq 1$, we find the following: (1) Orbits with fiducial periods of $P = 4$ yr and 40 yr could be spatially resolved and monitored. (2) For a 95% accuracy of $2 \mu\text{as}$ per monitoring epoch, sub-parsec values of a_{bin} could be accessed over a range of mass ratios notionally encompassing major ($q > \frac{1}{4}$) and minor ($q < \frac{1}{4}$) galaxy mergers. (3) If no reflex motion is detected for M_{pri} after 1(10) yr of monitoring, a SMBH binary with period $P = 4(40)$ yr and mass ratio $q > 0.01(0.003)$ could be excluded. This would suggest no present-day evidence for a past major merger like that recently simulated, where scouring by a $q \sim 1$ SMBH binary formed a stellar core with kinematic traits like those of NGC 4472. (4) Astrometric monitoring could independently check the upper limits on q from searches for continuous gravitational waves from NGC 4472.

Keywords: Active galactic nuclei (16); Early-type galaxies (429); Supermassive black holes (1663); Interferometry (808)

1. MOTIVATION

The merger of two galaxies, each hosting a supermassive black hole (SMBH) of mass $10^6 M_{\odot}$ or more, is expected to yield an SMBH binary. Eventually the orbit of the SMBH binary will shrink due to gravitational wave (GW) emission (Begelman et al. 1980). Such GW signatures are currently being sought with the Parkes Pulsar Timing Array (PPTA; Manchester et al. 2013; Shannon et al. 2015; Lasky et al. 2016), the European Pulsar Timing Array (Lentati et al. 2015; Babak et al. 2016; Desvignes et al. 2016), and the North American Nanohertz Observatory for Gravitational Waves (NANOGrav; Arzoumanian et al. 2018). It is also anticipated that such

GW signatures will be detected with the future Laser Interferometer Space Array (Amaro-Seoane et al. 2017).

In addition, searches are underway for the electromagnetic (EM) signatures of SMBH binaries. Decades of data seeking indirect EM signatures, such as periodicities in the optical emission-line velocities or photometric variability of active galactic nuclei (AGNs), have been used to identify candidate SMBH binaries. See Burke-Spolaor et al. (2019) and De Rosa et al. (2019) for recent reviews of all of the topics mentioned above.

One direct EM signature would be to spatially resolve and monitor the orbit of one or both members of an SMBH binary. Bansal et al. (2017) report possible evidence for orbital motion in the 7.3-pc binary in the radio galaxy 0402+379. But the estimated period spans millennia, making it difficult to acquire sufficient observables to solve for an orbit. EM strategies for studying tighter and more easily measured orbits are only now

being devised (D’Orazio & Loeb 2018; Safarzadeh et al. 2019; Dexter et al. 2020). These strategies rely upon recent or projected advances in interferometric techniques at millimeter (mm) or near-infrared wavelengths.

Here, we consider a strategy proposed by Safarzadeh et al. (2019) for continuum targets at Jansky (Jy) levels observable at 230 GHz (1.3 mm) with the Event Horizon Telescope (EHT; EHT Collaboration et al. 2019), and adapt it for the fainter, more abundant targets at milliJansky (mJy) levels that could be observed at 80 GHz (3.7 mm) with a next-generation Very Large Array¹ (ngVLA; Murphy et al. 2018).

Section 2 describes the selection of an example target, while Section 3 describes an observing strategy that capitalizes on a powerful, designed-in capability of the ngVLA at its highest resolutions, namely paired antenna calibration (Carilli & Holdaway 1999; Carilli et al. 2021). Section 4 explores the implications of high-resolution ngVLA observations for astrometric monitoring and for related tie-ins to galaxy evolution and to multimessenger astronomy in the context of GW observations. We close in Section 5 with a summary and conclusions. A preliminary version of this work appeared in Wrobel & Lazio (2021).

2. TARGET SELECTION

We focus on the early-type galaxy NGC 4472, the dominant galaxy in Virgo Subcluster B (e.g., Janowiecki et al. 2010; Arrigoni Battaia et al. 2012). Throughout we assume a distance of 16.7 Mpc, where 81.0 pc subtends 1'' (Blakeslee et al. 2009).

NGC 4472 may have experienced one or more galaxy mergers, as suggested from its overall slow rotation and its stellar core, which exhibits a substantial mass deficit, counter rotation and tangentially-biased orbits (e.g., Bettoni et al. 2001; Krajnovic et al. 2011; Emself et al. 2011; Thomas et al. 2014). Such core traits are linked to stellar scouring by an SMBH binary, a potential byproduct of a galaxy merger (e.g., Milosavljevic et al. 2002; Gualandris & Merritt 2008; Kormendy & Bender 2009). Finally, though somewhat fortuitous, Mingarelli et al. (2017) conduct a series of simulations to construct realizations of the local GW landscape. They find that NGC 4472 plausibly could host a SMBH binary and illustrate some of their results by considering it specifically.

High-resolution imaging of the low-luminosity AGN in NGC 4472 using the technique of very long baseline interferometry (VLBI) is available only at 5 GHz (6.0 cm)

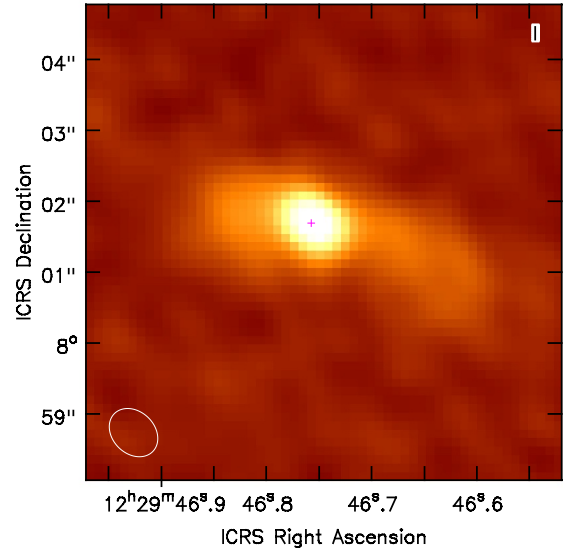


Figure 1. ALMA archival image of the emission at 98 GHz (3.1 mm) from the low-luminosity AGN in NGC 4472. The scale is 1'' = 81.0 pc (Blakeslee et al. 2009). The ellipse in the southeast corner shows the synthesized beam dimensions at FWHM of 0''.76 (62 pc) \times 0''.59 (48 pc) with an elongation position angle of 46°. The cross marks the location of the emission peak, which has a value of 2.92 mJy beam⁻¹. The white box in the northwest corner highlights the label *I* for the Stokes parameter.

and 8.4 GHz (3.6 cm) (Anderson & Ulvestad 2005; Nagar et al. 2005). The most constraining size information comes from the Very Long Baseline Array image at 8.4 GHz showing a 4-mJy source (Anderson & Ulvestad 2005). The diameter of the cm source has a full width at half maximum (FWHM) of less than 0.73 mas (0.059 pc). Attempts to probe smaller size scales, via time variability at 8.4 GHz and 15 GHz (2.0 cm) using the Very Large Array, were inconclusive (Anderson & Ulvestad 2005; Nagar et al. 2005).

Hydrodynamical simulations including radiative processes and SMBH feedback suggest that NGC 4472’s low-luminosity AGN can be understood as arising from jet-like outflows traced via synchrotron emission and launched from a radiatively-inefficient accretion inflow (e.g., Inayoshi et al. 2020).

3. NGVLA OBSERVATIONS

We adopt the ngVLA’s Long Baseline Array (LBA) component, which features ten sites and three 18 m antennas per site (Carilli et al. 2021). We assume an observing frequency of 80 GHz to match that assigned to notional continuum studies in the highest frequency band (Wrobel et al. 2020). The point spread function

¹ <https://ngvla.nrao.edu>

after tapering the natural weights is modelled² to have a FWHM of $PSF = 0.1$ mas (0.0081 pc).

To accrue a reasonable time on the target, one antenna per LBA site would observe the phase calibrator while the other two continuously observed NGC 4472 (Carilli & Holdaway 1999; Carilli et al. 2021). This capability is generally not available with current VLBI arrays, but has been designed into the ngVLA’s LBA component. After 4 hours on target with dual-polarization receivers and a bandwidth of 20 GHz per polarization, the thermal noise is modelled² to have a root-mean-square value of about $3 \mu\text{Jy beam}^{-1}$.

The overall astrometric accuracy of the ngVLA observation will have contributions from terms due to (i) the signal-to-noise ratio S/N on the target, $\sigma_{s/n}$; and (ii) the relative accuracy achieved via phase referencing, σ_{pr} . Regarding term (i), Figure 1 shows an image of NGC 4472 at 98 GHz (3.1 mm), obtained from the archives of the Atacama Large Millimeter/submillimeter Array (ALMA) using the Cube Analysis and Rendering Tool for Astronomy (CARTA).³ If the peak signal in Figure 1 is available to the ngVLA at 80 GHz, it would have a $S/N \sim 970$ and be localized with an associated accuracy of $\sigma_{s/n} = PSF/(1.665 \times S/N) \sim 0.1 \mu\text{as}$. This expression stems from equation (25) in Condon et al. (1998) and applies to Gaussian-based fitting.

Regarding term (ii), the phase referencing will be imperfect due to the different atmospheric conditions associated with two separations, that between the sky locations of the target and the phase calibrator, and that between the ground locations of the target antenna and the calibrator antenna (equation 13.128 of Thompson et al. 2017). To reach levels of $\sigma_{pr} \sim 1 \mu\text{as}$ at mm wavelengths, it is desirable to employ multiple phase calibrators whose sky locations are separated from the target by less than $1\text{--}2^\circ$ (Broderick et al. 2011; Reid & Honma 2014; Rioja & Dodson 2020). Several such calibrator candidates are already known for NGC 4472, one with a sub-degree separation.⁴ Some of the calibrator candidates appear to be adequately strong according to the ALMA Calibrator Source Catalog.⁵ Others could be briefly observed to assess their suitability. It is also desirable to closely pack the target and calibrator antennas per LBA site. Below, we assume that the overall astrometric accuracy of the ngVLA observation will be dominated by term (ii), with $\sigma_{pr} \sim 1 \mu\text{as}$.

4. IMPLICATIONS

4.1. Astrometric Monitoring

Following Safarzadeh et al. (2019), we examine how astrometric monitoring of NGC 4472 could constrain the reflex motion of the low-luminosity AGN’s primary SMBH of mass M_{pri} , as it is tugged on by a putative secondary SMBH of mass M_{sec} . These masses define a binary mass $M_{bin} = M_{pri} + M_{sec}$ and mass ratio $q = M_{sec}/M_{pri} \leq 1$. We allow q to vary. We adopt $M_{bin} = 2.4_{-0.1}^{+0.3} \times 10^9 M_\odot$ from Schutz & Ma (2016), which is the dynamically derived mass estimate from Rusli et al. (2013) but linearly scaled to an assumed distance of 16.7 Mpc (Blakeslee et al. 2009). Because early-type galaxies with larger SMBH masses are more likely to exhibit nuclear radio emission (e.g., Nyland et al. 2016), we assume that the mm emission from NGC 4472 is associated with its primary SMBH.

We assume a circular orbit for the SMBH binary and use Kepler’s third law to link the binary’s semimajor axis a_{bin} to its mass M_{bin} and orbital period P (equation (1) of Dexter et al. 2020). The reflex motion of M_{pri} as it orbits, with semimajor axis a_{pri} , about the binary’s center of mass is $a_{pri} = a_{bin} \times q/(1+q)$ (equation (1) of Safarzadeh et al. 2019). We recast this as

$$a_{bin} = a_{pri} \times (1+q)/q. \quad (1)$$

Suppose that ngVLA astrometry of the low-luminosity AGN could achieve a 95% accuracy of $2 \mu\text{as}$ for each epoch in a monitoring sequence. Then the reflex constraint per epoch would become $a_{pri} = 2 \mu\text{as} \times 81.0 \text{ pc}/10^6 \mu\text{as} = 0.00016 \text{ pc}$. Inserting this value into equation (1) then defines how a_{bin} can be related to q . This behavior is shown as the navy diagonal line in Figure 2. The parameter space to the right of this line is accessible via ngVLA monitoring of NGC 4472 with the adopted astrometric accuracy. The parameter space to the left of this line is inaccessible.

A possible complication regarding the ngVLA monitoring deserves mention: Su et al. (2019) suggest that NGC 4472 is moving northward, relative to its surrounding X-ray-emitting gas, with a velocity $v_{X\text{-ray}} \sim 450_{-143}^{+192} \text{ km s}^{-1}$. A putative SMBH binary would share this velocity. Projection effects are not known but if this velocity is purely in the plane of the sky, it would have a secular proper motion $\mu_{X\text{-ray}} \sim 5.7_{-1.8}^{+2.4} \mu\text{as yr}^{-1}$. ngVLA monitoring may reveal such a secular motion, upon which any reflex motion of M_{pri} would be superposed. Such a complication can be handled as for Sgr A*, where proper motion studies exclude any oscillatory reflex signals (Reid & Brunthaler 2004).

In contrast to numerous prior studies that aim to detect the cm emission from both SMBHs in the rem-

² <https://gitlab.nrao.edu/vrosero/ngvla-sensitivity-calculator>

³ <https://doi.org/10.5281/zenodo.4905459>

⁴ <http://www.vlba.nrao.edu/astro/calib/>

⁵ <https://almascience.nrao.edu/sc/>

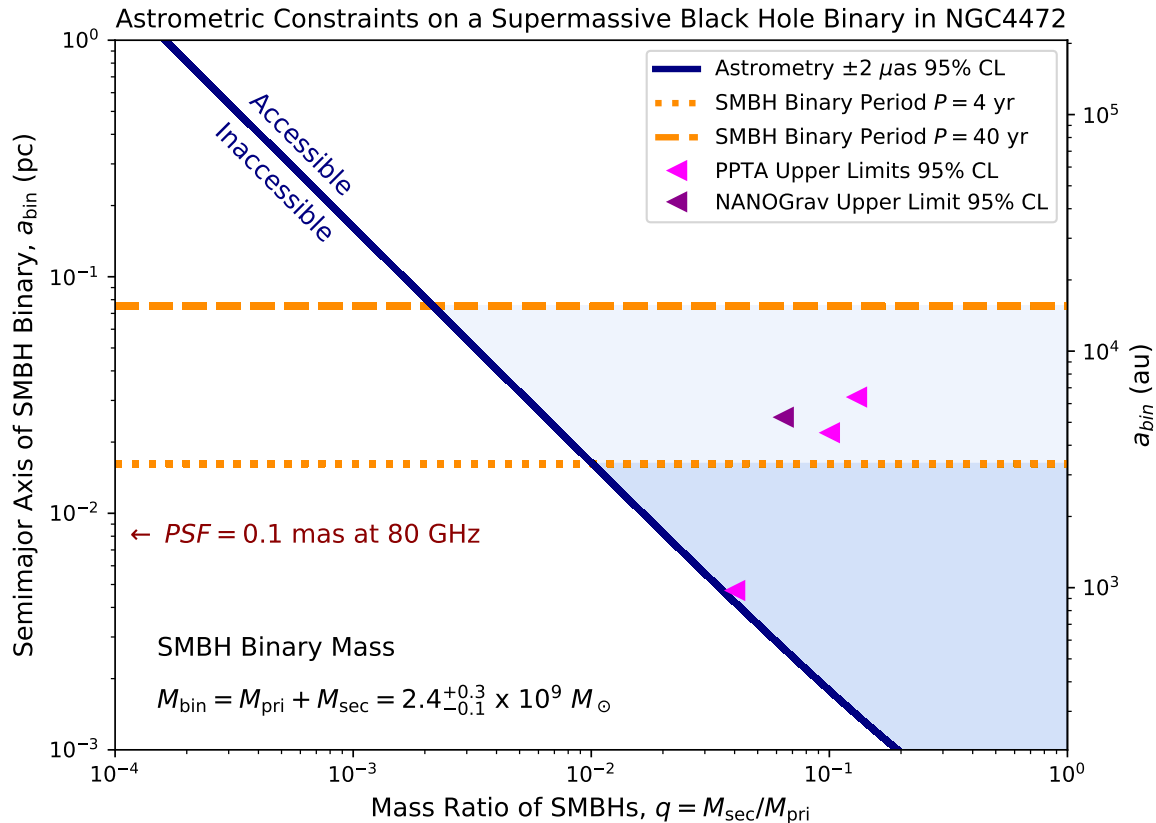


Figure 2. Parameter space for a_{bin} and q for a putative SMBH binary in the early-type galaxy NGC 4472. M_{bin} is from Rusli et al. (2013). The region to the right of the navy diagonal line is accessible with ngVLA astrometric monitoring at 80 GHz with the labelled accuracy. The associated PSF of the ngVLA Long Baseline Array (LBA) is marked for reference. The GW constraints from the PPTA are tabulated in Schutz & Ma (2016), while that from NANOGrav is derived from Arzoumanian et al. (2021). All quantities invoke the Blakeslee et al. (2009) distance of 16.7 Mpc.

nant of a galaxy merger (Burke-Spolaor et al. 2019; De Rosa et al. 2019, and references therein), our strategy needs detectable mm emission from only one SMBH. Also unlike those studies, our strategy can leverage the frequency coverage, angular resolution, and sensitivity of the ngVLA to conduct searches well into the regime in which a SMBH binary emits GWs, a topic further developed in Section 4.3.

4.2. Tie-Ins to Galaxy Evolution

Figure 2 shows the values of a_{bin} associated with fiducial SMBH binary periods of $P = 4$ yr and $P = 40$ yr. Astrometric monitoring through a quarter of a period would be sufficient to constrain the range of mass ratios q allowed for the period. As is evident from Figure 2, orbits with these periods could be spatially resolved by the ngVLA.

If no reflex motion is detected for M_{pri} after 1 yr of ngVLA monitoring of NGC 4472, a SMBH binary with

period $P = 4$ yr and mass ratio $q > 0.01$ could be excluded. The darker blue shading in Figure 2 indicates where SMBH binaries with shorter periods and higher mass ratios could also be excluded. This exclusion is based on ngVLA astrometry and applies even for orbits that are not spatially resolved with the ngVLA.

If reflex motion remains undetected after a decade of ngVLA monitoring of NGC 4472, a SMBH binary with $P = 40$ yr and $q > 0.003$ could be excluded. Shorter periods with higher mass ratios could also be excluded, as shown by the lighter blue shading in Figure 2.

Below, we cast such constraints on q , the mass ratio of the SMBH binary, in terms of traits traceable to galaxy merger events as NGC 4472 is assembled. The close coupling between galaxy and SMBH masses makes it reasonable to assume that q for a SMBH binary will be similar to the mass ratio of the two progenitor galaxies which, after merging, give rise to the SMBH binary. Major galaxy mergers involve progenitors of comparable

mass, whereas minor galaxy mergers involve progenitors of dissimilar mass (e.g., [Volonteri et al. 2003](#)). Following the common practice of separating major and minor mergers at a mass-ratio boundary of about $\frac{1}{4}$, Figure 2 implies access to both types of galaxy mergers.

4.2.1. Large q Values

We first examine whether large values for the mass ratio q could be relevant to NGC 4472. [Rantala et al. \(2019\)](#) use numerical simulations to show that the dissipationless, major merger of two galaxies can yield a SMBH binary that builds a stellar core, with tangentially biased orbits, that is counter rotating relative to the surrounding merger remnant, a massive early-type galaxy.

While not meant to model NGC 4472 specifically, the simulations of [Rantala et al. \(2019\)](#) do appear to offer a potential explanation for the kinematics of its stellar core (see Section 2). In this context, ngVLA astrometric monitoring of NGC 4472 would be seeking present-day evidence for the SMBH binary at high q and on sub-parsec scales (Figure 2).

A dissipationless scouring process shrinks the binary orbit on a timescale $t_{\text{sc}} \propto a_{\text{bin}}^{-1}$, slow compared to the timescale $t_{\text{gw}} \propto a_{\text{bin}}^{+4}$ for orbit shrinkage driven by GW emission (e.g., Supplementary Figure 5; [Mingarelli et al. 2017](#)). Stated differently, the residence time over which a SMBH binary might be detected via astrometry is longer than the residence time over which it might be detected via GW emission.

4.2.2. Small q Values

Small q values could also be relevant to NGC 4472, given observational evidence suggesting it has built up some of its size and mass by accreting satellite galaxies (e.g., [Janowiecki et al. 2010](#); [Arrigoni Battaia et al. 2012](#)). As noted by [Kormendy & Ho \(2013\)](#), typical merger trees involve galaxies that could transport their own SMBHs inward. For example, an in-coming SMBH with a mass $M_{\text{sec}} \sim 2 \times 10^7 M_{\odot}$ could lead to a SMBH binary with a mass ratio $q \sim 0.01$, accessible astrometrically according to Figure 2.

4.3. Tie-Ins to GW Findings

NGC 4472 is sufficiently close that, if it hosts a SMBH binary, any GW emissions from that binary might be detectable by current or near-future pulsar timing arrays. As such, there is the possibility to obtain independent checks on certain parameters or more comprehensive information about the system than would be available from only electromagnetic (ngVLA) or gravitational wave (pulsar timing) measurements.

ngVLA astrometric monitoring could independently check the GW-based upper limits on q plotted in Figure 2 for NGC 4472, provided the GW findings invoke the same distance and SMBH binary mass adopted from [Schutz & Ma \(2016\)](#) for the astrometry. For the PPTA, the q values in Figure 2 are as tabulated by, and thus consistent with, the [Schutz & Ma \(2016\)](#) distance and SMBH binary mass.

For NANOGrav, we focus first on a GW frequency of 8 nanoHz (nHz), at which the most constraining limits on GW strain can be set ([Aggarwal et al. 2019](#); [Arzoumanian et al. 2021](#)). From equation (1) of [Schutz & Ma \(2016\)](#), we set a 95% upper limit on the associated chirp mass of $M_{\text{chi}} < 0.44 \times 10^9 M_{\odot}$ for our adopted distance to NGC 4472. We then insert the ratio of the chirp mass to our adopted binary mass into equation (5) of [Schutz & Ma \(2016\)](#) to set the 95% upper limit of $q < 0.064$ that we plot in Figure 2. These upper limits on M_{chi} and q are higher than those shown near 8 nHz in Figure 2 of [Arzoumanian et al. \(2021\)](#); such differences arise because that study adopts a cosmic-flow distance which is larger than the [Schutz & Ma \(2016\)](#) distance.

The NANOGrav search spans a GW frequency range of 2.8 nHz to 317.8 nHz ([Aggarwal et al. 2019](#)). This range corresponds to orbital periods of a putative SMBH binary from $P = 22.6$ yr to $P = 0.2$ yr, equivalent to $a_{\text{bin}} = 10600$ au to $a_{\text{bin}} = 453$ au for $M_{\text{bin}} = 2.4 \times 10^9 M_{\odot}$ ([Schutz & Ma 2016](#)). GW-derived separations are so small that they are often expressed not in pc, but in au. (An au axis is provided in Figure 2.) The PSF adopted for the ngVLA astrometry of NGC 4472 corresponds to 1670 au, making it complementary to and midway within the range of separations constrained by [Aggarwal et al. \(2019\)](#). Those GW constraints degrade significantly below about 5 nHz, due to the 11 yr data span. Future observations, potentially enhanced with ngVLA pulsar timing data ([Chatterjee et al. 2018](#)), will improve the NANOGrav constraints, and extend them to lower GW frequencies or longer orbital periods.

Finally, most GW analyses have been conducted assuming circular orbits. As might be expected, for a SMBH binary on an elliptical orbit, GWs are emitted not only at a frequency determined by the orbital period but also at higher harmonics. The consequence is that there can be a penalty in signal-to-noise ratio if a circular orbit is assumed, but the orbit is elliptical ([Huerta et al. 2015](#); [Taylor et al. 2016](#)). This penalty particularly applies if the orbital period is shorter than $1/T$, where T is the data span for the pulsar timing. Thus, the limits quoted above for NGC 4472 become less constraining if one considers elliptical orbits, particularly those at the higher GW frequencies probed by NANOGrav. If

ngVLA astrometry of NGC 4472 were to suggest that it contained a SMBH binary on an elliptical orbit, improved limits on the chirp mass M_{chi} or mass ratio q could likely be obtained.

5. SUMMARY AND CONCLUSIONS

A direct EM signature of an SMBH binary would be to spatially resolve and monitor the orbit of one or both of its members. To that end, we adapted the strategy of Safarzadeh et al. (2019) for EHT targets at 230 GHz to the more abundant targets observable with the ngVLA at 80 GHz. The strategy involves astrometric monitoring to trace the reflex motion of the binary’s primary SMBH as it is tugged on by the secondary SMBH. Only one member of the binary needs to have detectable mm emission.

Picking the early-type galaxy NGC 4472 as an example and casting the circular orbit of a putative SMBH binary in terms of its period P , semimajor axis a_{bin} , and secondary-to-primary mass ratio q , we found the following:

1. Orbits with fiducial periods of $P = 4$ yr and 40 yr could be spatially resolved and monitored with the ngVLA.
2. For a 95% accuracy of $2 \mu\text{as}$ per ngVLA monitoring epoch, sub-parsec values of a_{bin} could be accessed over a range of mass ratios notionally encompassing major ($q > \frac{1}{4}$) and minor ($q < \frac{1}{4}$) galaxy mergers.
3. If no reflex motion was detected for the primary after 1(10) yr of ngVLA monitoring, a SMBH binary with period $P = 4(40)$ yr and mass ratio $q > 0.01(0.003)$ could be excluded. This would suggest no present-day evidence for a past major

merger like one recently simulated, wherein scouring by a $q \sim 1$ SMBH binary formed a stellar core with the kinematic properties of NGC 4472’s stellar core.

4. Astrometric monitoring with the ngVLA could independently check the upper limits on q for NGC 4472 from searches for continuous gravitational waves with the PPTA and NANOGrav.

ACKNOWLEDGMENTS

We thank the reviewer for their helpful and timely report.

The NRAO is a facility of the National Science Foundation (NSF), operated under cooperative agreement by Associated Universities, Inc. (AUI). The ngVLA is a design and development project of the NSF operated under cooperative agreement by AUI.

The NANOGrav project receives support from NSF Physics Frontiers Center award number 1430284. Part of this research was carried out at the Jet Propulsion Laboratory, California Institute of Technology, under a contract with the National Aeronautics and Space Administration.

This paper makes use of the following ALMA data: ADS/JAO.ALMA# 2015.1.00926.S. ALMA is a partnership of ESO (representing its member states), NSF (USA) and NINS (Japan), together with NRC (Canada), MOST and ASIAA (Taiwan), and KASI (Republic of Korea), in cooperation with the Republic of Chile. The Joint ALMA Observatory is operated by ESO, AUI/NRAO and NAOJ.

Software: astropy (Astropy Collaboration et al. 2018), CARTA (Wang et al. 2020)

REFERENCES

- Aggarwal, K., Arzoumanian, Z., Baker, P. T., et al. 2019, ApJ, 880, 116
- Amaro-Seoane, P., Audley, Babak, S., et al. 2017, arXiv:1702.00786
- Anderson, J. M., & Ulvestad, J. S. 2005, ApJ, 627, 674
- Arrigoni Battaia, F., Gavazzi, G., Fumagalli, M., et al. 2012, A&A, 543, A112
- Arzoumanian, Z., Baker, P. T., Brazier, A., et al. 2018, ApJ, 859, 47
- Arzoumanian, Z., Baker, P. T., Brazier, A., et al. 2021, ApJ, 914, 121
- Astropy Collaboration et al. 2018, AJ, 156, 123
- Babak, S., Petiteau, A., Sesana, A., et al. 2016, MNRAS, 455, 1665
- Bansal, K., Taylor, G. B., Peck, A. B., Zavala, R. T., & Romani, R. W. 2017, ApJ, 843, 14
- Begelman, M. C., Blandford, R. D., & Rees, M. J. 1980, Nature, 287, 307
- Bettoni, D., Galletta, G., & Prada, F. 2001, A&A, 374, 83
- Blakeslee, J. P., Jordan, A., Mei, S., et al. 2009, ApJ, 694, 556
- Broderick, A. E., Loeb, A., & Reid, M. J. 2011, ApJ, 735, 57

- Burke-Spolaor, S., Taylor, S. R., Charisi, M., et al. 2019, *Astronomy and Astrophysics Review*, 27, 5
- Carilli, C., & Holdaway, M. 1999, *Radio Science*, 34, 817
- Carilli, C., Mason, B., Rosero, V., et al. 2021, ngVLA Memo. #92
- Chatterjee, S., et al. 2018, in ASP Conf. Ser. 517, *Science with a Next Generation Very Large Array*, ed. E. J. Murphy et al. (San Francisco, CA: ASP), 751
- Condon, J. J., Cotton, W. D., Greisen, E. W., et al. 1998, *AJ*, 115, 1693
- De Rosa, A., Vignali, C., Bogdanovic, T., et al. 2019, *New Astronomy Reviews*, 86, 101525
- Desvignes, G., Caballero, R. N., Lentati, L., et al. 2016, *MNRAS*, 458, 3341
- Dexter, J., Lutz, D., Shimizu, T. T., et al. 2020, *ApJ*, 905, 33
- D’Orazio, D. J., & Loeb, A. 2018, *ApJ*, 863, 185
- EHT Collaboration et al. 2019, *ApJL*, 875, L1
- Emsellem, E., Cappellari M., Krajnovic, D., et al. 2011, *MNRAS*, 414, 888
- Gualandris, A., & Merritt, D. 2008, *ApJ*, 678, 780
- Huerta, E. A., McWilliams, S. T., Gair, J. R., & Taylor, S. R. 2015, *PhRvD*, 92, 063010
- Inayoshi, K., Ichikawa, K., & Ho, L. C. 2020, *ApJ*, 894, 141
- Janowiecki, S., Mihos, J. C., Harding, P. 2010, *ApJ*, 715, 972
- Kormendy, J., & Bender, R. 2009, *ApJL*, 691, L142
- Kormendy, J., & Ho, L. C. 2013, *ARA&A*, 51, 511
- Krajnovic, D., Emsellem, E., & Cappellari, M., et al. 2011, *MNRAS*, 414, 2923
- Lasky, P. D., Mingarelli, C. M. F., Smith, T. L., et al. 2016, *Phys. Rev. X*, 6(1), 011035
- Lentati, L., Taylor, S. R., Mingarelli, C. M. F., et al. 2015, *MNRAS*, 453, 2576
- Manchester, R. N., Hobbs, G., Bailes, M., et al. 2013, *PASA*, 30, e017
- Milosavljevic, M., Merritt, D., Rest, A., & van den Bosch, F. C. 2002, *MNRAS*, 331, L51
- Mingarelli, C. M. F., Lazio, T. J. W., Sesana, A., et al. 2017, *Nature Astronomy*, 1, 886
- Murphy, E. J., Bolatto, A., Chatterjee, S., et al. 2018, in ASP Conf. Ser. 517, *Science with a Next Generation Very Large Array*, ed. E. J. Murphy et al. (San Francisco, CA: ASP), 3
- Nagar, N. M., Falcke, H., & Wilson, A. S. 2005, *A&A*, 435, 521
- Nyland, K. E., Young, L. M., Wrobel, J. M., et al. 2016, *MNRAS*, 458, 2221
- Rantala, A., Johansson, P. H., Naab, T., Thomas, J., & Frigo, M. 2019, *ApJL*, 872, L17
- Reid, M. J., & Brunthaler, A. 2004, *ApJ*, 616, 872
- Reid, M. J., & Honma, M. 2014, *ARA&A*, 52, 339
- Rioja, M. J., & Dodson, R. 2020, *Astronomy and Astrophysics Review*, 28, 6
- Rusli, S. P., Thomas, J., Saglia, R. P., et al. 2013, *AJ*, 146, 45
- Safarzadeh, M., Loeb, A., & Reid, M. 2019, *MNRAS*, 488, L90
- Schutz, K., & Ma, C.-P. 2016, *MNRAS*, 459, 1737
- Shannon, R. M., Ravi, V., Lentati, L. T., et al. 2015, *Science*, 349, 1522
- Su, Y., Kraft, R. P., Nulsen, P. E. J., et al. 2019, *ApJ*, 158, 6
- Taylor, S. R., Huerta, E. A., Gair, J. R., & McWilliams, S. T. 2016, *ApJ*, 817, 70
- Thomas, J., Saglia, R. P., Bender, R., Erwin, P., & Fabricius, M. 2014, *ApJ*, 782, 39
- Thompson, A. R., Moran, J. M., & Swenson, G. W. 2017, *Interferometry and Synthesis in Radio Astronomy* (New York, NY: John Wiley & Sons, Inc.), 710-711
- Volonteri, M., Haardt, F., & Madau, P. 2003, *ApJ*, 582, 559
- Wang, K.-S., Comrie, A., Harris, P., et al. 2020, in ASP Conf. Ser. 527, *Astronomical Data Analysis Software and Systems XXIX*, ed. Roberto Pizzo et al. (San Francisco, CA: ASP), 213
- Wrobel, J. M., Mason, B. S., & Murphy, E. J. 2020, NRAO Doc. #: 020.10.15.05.10-0002-REP, Revision A
- Wrobel, J. M., & Lazio, T. J. W. 2021, ngVLA Memo. #90, arXiv:2108.07341